Performance-based seismic assessment of shape memory alloy reinforced bridge pier considering combined peak and residual deformations

B. Shrestha & H. Hao

Dept. of Civil Engineering, Curtin University, Bentley, Australia.

C. Li & H.N. Li

Faculty of Infrastructure Engineering, Dalian University of Technology, Dalian, China.

ABSTRACT: Using super-elastic Shape Memory Alloy (SMA) reinforcements at plastic hinge regions of bridge piers could significantly reduce residual displacement due to their unique shape recovery characteristics. However, previous studies have shown that peak deformation of the SMA reinforced piers could be higher due to the relatively lower modulus of elasticity of SMA bars and their lower hysteretic energy dissipation capacity. Therefore, it is essential to consider both the peak and the residual deformation collectively while assessing the performance of SMA bridge piers. In this paper, a recently formulated probabilistic performance-based seismic assessment methodology that collectively considers the peak and the residual deformations is applied to evaluate the performance of SMA reinforced bridge piers. Joint fragility curves expressing the probability of exceedance of performance level defined by pair of peak and residual deformations are utilized to evaluate the performance of SMA reinforced bridge piers subjected to a suite of 30 near-fault ground motions. The results are then compared with the performance of steel reinforced bridge piers. The study revealed that SMA bridge pier has lower probability of exceeding higher damage levels defined by the joint maximum-residual deformations.

1 INTRODUCTION

Reinforced concrete (RC) bridge piers with high ductility capacity are used in highly seismic active regions to avoid collapse during strong ground shakings. During the previous earthquakes, this design philosophy resulted in prevention of collapse of many structures. However, it was observed that ductile RC structures that avoided the collapse due to the large inelastic deformations could sustain large residual deformation following an extreme earthquake event. During past major earthquake, such as Kobe 95, Northridge 94, Christchurch 2011, numerous structures (buildings and bridges) had to be demolished due to the large residual deformations making it impossible to return to their initial position. Consequently, there is a consensus among the researchers and practising engineers on the importance of residual deformations on the seismic performance and post-earthquake functionality of bridges (Saiidi and Aradakani 2012, Ramirez and Miranda 2012). Recently significant research have been made to improve the seismic performance of the bridges using advanced structure systems with re-centering properties, such as unbonded post-tensioned bridge piers or superelastic SMA reinforced piers.

This paper focuses on the performance-based assessment of superelastic SMA bridge piers. SMA reinforcement is applied at plastic hinge regions of the bridge piers to improve residual displacement performance and to reduce the cost of the composite bridge pier. Due to its unique ability to sustain large deformation and return to their original shape on stress removal superelastic SMA have found significant application in civil engineering structures in the recent years. Though a large number of alloys have been investigated for shape memory behaviour, NiTi (Nickel Titanium) based alloys are the most widely used due to several advantages such as large strain recovery, high energy dissipation and excellent resistance to corrosion. Many recent studies (Saiidi and Wang 2006, Saiidi et al. 2009, Youssef et al. 2008, Cruz and Saiidi 2012) have experimentally explored the effectiveness of superelastic SMA reinforcement at plastic hinge area of RC elements. While others (Billah and Alam

2014, Tazarv and Saiidi 2013, 2014, Shrestha et al. 2015, Shrestha and Hao, 2015) focused on numerical analysis to investigate the performance of the superelastic SMA reinforced concrete structures. Exponentially increasing numbers of research in recent on the application of superelastic SMA reinforced RC structures demonstrate the attractiveness of SMA reinforcement as an alternative to conventional steel reinforcement.

Recently the earthquake engineering community has been focusing attention on the performance-based engineering approaches in order to predict and better manage the post-earthquake functionality and conditions of structures. Earlier guidelines (FEMA 273) usually focused on response indices based on peak responses and little attention was given to the residual state. To include residual deformation to the performance level Pampanin et al. (2003) and Christopolous et al. (2003) proposed Residual Deformation Damage Index (RDDI) as an additional performance indicator. Pampanin et al. (2002) further developed the study by proposing the use of a three-dimensional performance matrix that combines two dependent variables Maximum Drift (MD) and Residual Drift (RD). Recently, Uma et al. (2010) formulated a probabilistic framework of the aforementioned performance based approach including MD and RD. In this paper, the probabilistic framework proposed in the latter study is applied to investigate the performance of typical RC bridge piers with superelastic SMA reinforcement. Using the joint fragility curve for MD and RD the likelihood of seismic demand exceeding the predefined damage limits at a chosen seismic excitation level are identified for bridge piers with superelastic SMA and steel reinforcements. No such study of using combined MD and RD response indices to define the performance to super elastic SMA reinforced bridge piers are found in the literature yet. As MD and RD are correlated variables, separate handling to these two variables may not provide a conclusive outcome. A suite of ground motion with 30 near-fault ground motions with directivity pulses are used to generate the fragility curves for SMA and steel RC bridge piers.

2 3D PERFORMANCE MATRIX

In the performance based earthquake engineering framework, a performance objective is typically defined when a set of structural performance level is coupled with intensity of seismic input. These performance levels are usually defined by single measures of peak response. Pampanin et al. (2002, 2003) proposed a performance measure as a combination of MD and RD in the format of performance matrix. The elements of the matrix are thereby conveniently identified as performance level defined by the pair of RD and MD. For different seismic intensities this results in a full three-dimensional performance domain as presented in Figure 1 (a). For a given seismic intensity, the performance matrix consists of a mask of pre-defined performance domains (on the X-Y pane) describing Performance Levels, PL (i, j), defined by the combination MD, with index i and RD, with index j as shown in Figure 1 (b).

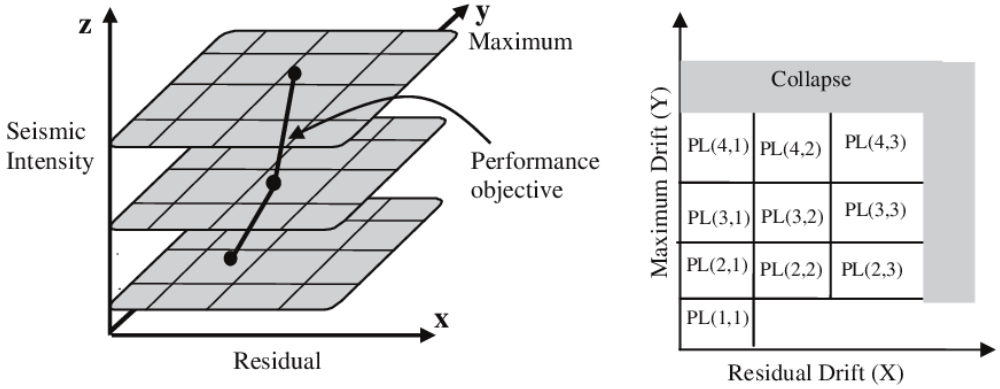

Figure 1. 3D performance matrix considering MD and RD indices (Pampanin et al. 2002, 2003).

Uma et al. (2010) extended the above described 3D matrix approach to compute a performance levels as a function of the combined probability of MD and RD by defining a probabilistic seismic demand

model. The probabilistic seismic demand model allows the estimation of experiencing a given combination of MD and RD conditioned on the level of ground motion intensity. Within the proposed probabilistic procedure, the probability of damage measure conditioned on Intensity Measure (IM) is expressed as

$$P[DM / IM] = \int\int P[DM / EDP_{RD,MD}] / \mathrm{dP}[\mathrm{EDP}_{RD,MD} / \mathrm{IM}] \quad (1)$$

where $P[DM/EDP_{RD,MD}]$ is the probability of a specific DM (Damage Measure) associated with a performance level determined by the pair of EDP (Engineering Demand Parameter) values and $dP[EDP_{RD,MD}/IM]$ represents the probability density function of EDPs conditioned on IM. Equation 1 is used to arrive at fragilities of combined performance levels conditioned on the joint occurrence of two EDPs. Detailed discussion on the methods of calculating fragility curves using combined performance levels is presented in Uma et al. (2010).

3 BRIDGE PIER MODEL

3.1 Description of bridge pier

To access the seismic performance of SMA RC bridge pier a typical Californian bridge pier with the height of 15 m is analysed. The details of the bridge piers and numerical model are presented in Figure 2. The diameter of the bridge piers is 1.8 m. The steel RC piers are reinforced with 64-32mm diameter (rebar ratio 2.02%) steel bars and SMA RC piers are reinforced with 74-32mm diameter (rebar ratio 2.34%) SMA rebars. The area of the rebar is adjusted for the two piers so that the peak moment capacities of the both piers are identical. All other geometrical features for the bridge piers are the same. To reduce the cost of the SMA RC piers, the SMA rebars are provided only in the plastic hinge region of the pier and connected using mechanical couplers with the steel rebars outside the plastic hinge region. The plastic hinge length, L_p is calculated according to the following relationship (Paulay and Preistley 1992);

$$L_p = 0.08L + 0.022 d_b f_y \quad (2)$$

where L is the length of the member in mm, d_b represents the bar diameter in mm, f_y is the yield strength of the rebars in MPa. SMA RC piers are designed to ensure that SMA rebars inside the plastic hinge region yields before the yielding of the steel bars it is connected to. Compressive strength of the concrete and yield strength of the rebars are 35 MPa and 414 MPa, respectively. The mechanical properties of the SMA rebars are given in Table 1.

Table 1. Mechanical properties of SMA rebar.

Material	Property	Value
Super-elastic SMA	Modulus of Elasticity (MPa)	48300
	Austenite to martensite starting stress, f_{sm} (MPa)	379
	Austenite to martensite finishing stress, f_{fm} (MPa)	405
	Martensite to austenite starting stress, f_{sa} (MPa)	180
	Martensite to austenite finishing stress, f_{fa} (MPa)	100
	Super-elastic plateau strain (%)	5.5

3.2 Numerical model

The numerical modelling of the bridge piers are conducted using Seismostruct software (Seismostruct 2012). Displacement based nonlinear beam column elements discretized into 12 finite element frames are used to model the piers. Fibre element approach is employed to represent the distribution of inelasticity along the length and cross-sectional area of the member. The fibre section used for the column is discretised into core fibre for confined concrete, cover fibre for unconfined concrete and

steel/SMA fibre for reinforcement bars. SMA bars are modelled using uniaxial model of superelastic SMA programmed and implemented in Seismostruct by Fugazza (2003) following the constitutive relationship proposed by Auricchio and Sacco (1997). The model is capable of describing the force-deformation behaviour of superelastic SMAs at a constant temperature. Bond slip effect in the longitudinal steel bar is considered using the modified Wehbe's method (Wehbe et al. 1999, Vosoogi and Saiidi 2010) and included in the form of moment-rotation spring at the end of the column using zero-length link element. Slippage of SMA rebars inside the mechanical coupler is included using the bond-slip relationship from the experiment of Alam et al. (2010) and Billah and Alam (2012). The details of finite element are presented in Figure 1. The previous investigation from the authors (Shrestha and Hao 2015) validated the numerical model using the shake table studies conducted by Saiidi and Wang (2006).

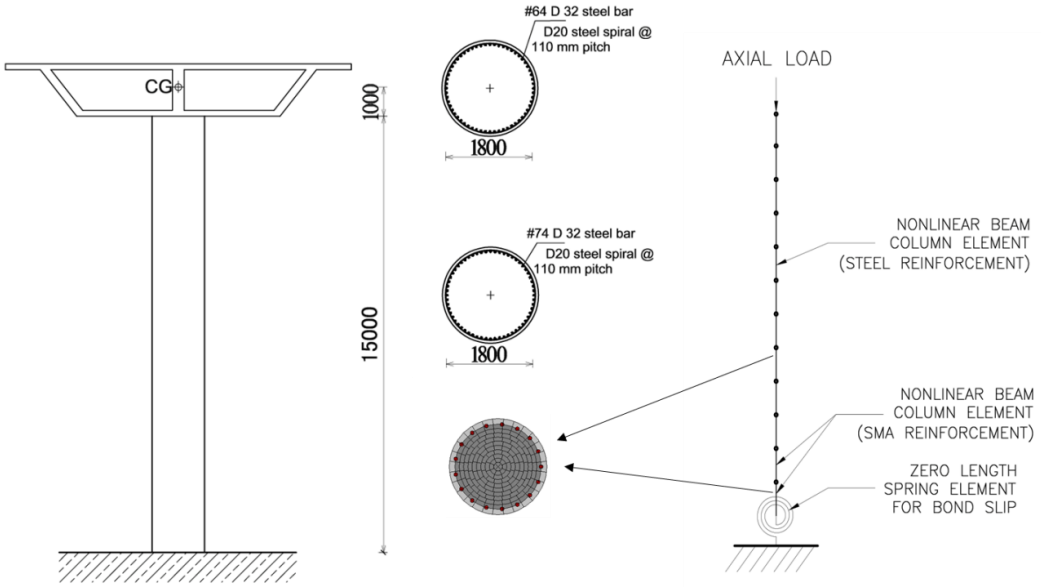

Figure 2. Geometrical detail and numerical model of the bridge pier (dimension in mm).

4 GROUND MOTIONS

Recent earthquake records have shown that in the proximity of an active fault, ground motions are significantly affected by the faulting mechanism, direction of rupture propagation relative to the site, for e.g., forward directivity. These near-fault ground motions often contain a strong and long period velocity pulse that could cause severe structural damage. These types of ground motions may generate high demands that force the structures to dissipate this input energy with a few large displacement excursions. Previous investigations (Phan et al. 2007, Choi et al. 2010) found that the most unique measured response characteristic of RC bridge piers subjected to near-fault ground motions was the significant residual displacement even under moderate motions. A suite of 30 near fault ground motions are used to access the combined MD and RD performance of SMA RC and steel RC bridge piers. All the ground motions were recorded within 15 km from the causative fault rupture plane and contained strong velocity pulse. The details of the ground motions are provided in Table 2. All the ground motions were recorded at site C and D according to the NEHRP provisions (FEMA 273). The normalized mean spectrum of the selected ground motions closely match the design spectrum for the selected bridge site.

5 NUMERICAL ANALYSIS

5.1 Seismic response analysis

Incremental Dynamic Analyses (IDA) using the ground motion suite is performed for SMA RC and steel RC piers. The seismic intensity levels are increased by scaling up the PGA to 10 different levels,

from 0.15 to 1.5 g. Figure 4 shows the time history response plot for SMA RC and steel RC bridge pier. SMA RC bridge pier showed a significantly better response in terms of recovering the drift at the end of the ground motion, indicated by the lower RD. Though the MD of the SMA RC pier is slightly higher than that of Steel RC pier due to the lower stiffness and lower hysteretic energy dissipation, the residual displacement of the pier is more than 10 times less for the presented case. The MD and RD are then calculated for the 30 ground motions at ten intensities.

Table 2. Details of near-fault ground motions used.

Record No	Year	Earthquake	M_W	Station	Dist. (km)	Site Class*	PGA (g)
1	1979	Imperial-Valley	6.5	Brawley Airport	11.3	D	0.16
2	1979	Imperial-Valley	6.5	El Centro Array #3	13.8	D	0.22
3	1979	Imperial-Valley	6.5	El Centro Diff. Array	5.6	D	0.35
4	1979	Imperial-Valley	6.5	El Centro Imp. Co. Cent.	7.6	D	0.23
5	1979	Imperial-Valley	6.5	Holtville Post Office	8.8	D	0.22
6	1999	Kocaeli	7.4	Duzce	11.0	D	0.31
7	1989	Loma Prieta	7.0	Gilroy STA #2	4.5	D	0.37
8	1989	Loma Prieta	7.0	Gilroy STA #3	6.3	D	0.37
9	1994	Northridge	6.7	Rinaldi Rec. Stn.	8.6	D	0.84
10	1994	Northridge	6.7	Slymar Con. Sta	6.1	D	0.83
11	1979	Imperial-Valley	6.5	El Centro Array #7	3.1	D	0.46
12	1994	Northridge	6.7	Jensen Filt. Plant	6.2	D	0.42
13	1994	Northridge	6.7	Newhall LA Fire Stn.	7.1	D	0.58
14	1994	Northridge	6.7	Sylmar Olive View Hos.	6.4	D	0.84
15	1987	Superstition Hills	6.4	Parachute Test Site	0.7	D	0.45
16	1994	Northridge	6.7	Newhall Pico Canyon	7.1	D	0.45
17	1989	Loma Prieta	7.0	Corralitos	5.1	D	0.64
18	2004	Parkfield	6.4	Cholame 1E	6.5	D	0.47
19	2004	Parkfield	6.4	Cholame 5W (Sta 5)	10.0	D	0.21
20	2004	Parkfield	6.4	Fault Zone 1	3.4	D	0.50
21	2004	Parkfield	6.4	Gold Hill 1W	0.8	D	0.13
22	1992	Cape Mendocino	7.1	Petrolia, General Store	15.9	C	0.66
23	1992	Erzincan	6.7	Erzincan	2.0	C	0.50
24	1999	Chi-Chi	7.6	CHY028	7.3	D	0.82
25	1999	Chi-Chi	7.6	CHY101	11.1	D	0.44
26	1999	Chi-Chi	7.6	TCU049	4.5	D	0.25
27	1999	Chi-Chi	7.6	TCU053	6.7	D	0.14
28	1979	Imperial-Valley	6.5	El Centro Array #4	6.8	D	0.36
29	1995	Kobe	6.7	KJMA	0.6	C	0.82
30	1979	Loma Prieta	7.0	Gilroy STA #2	10.9	C	0.36

*NEHRP Site Classifications: (C for Vs = 360 to 760 m/s), (D for Vs = 180 to 360 m/s).

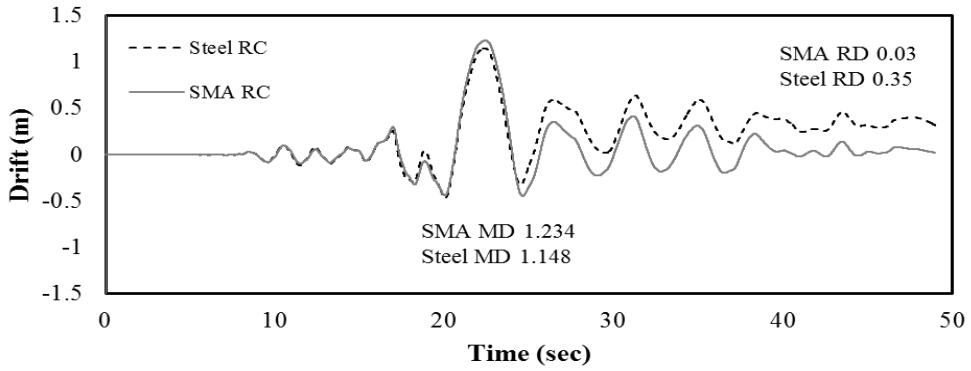

Figure 3. Displacement time history of the bridge piers analysed at PGA 0.6g of record 25.

5.2 **Definition of Limit States**

Five different damage limit states based on MD and RD are defined as shown in Table 3. Matrix based Performance Levels (PLs) are defined based on the combined MD and RD performance of the piers. For the limit states based on MD accepted values based on previous literatures (Kim and Shinozuka 2004, Dutta and Mander 1999) are used. Additionally, five damage states based on the RD are also defined based on the previous investigations (O'Brien et al. 2007, Shrestha and Hao 2015) and bridge design codes (Japan Road Association 2006). A threshold of 0.25% for RD is defined below which the structure will meet the serviceability requirement providing full functionality. While a RD of 1% is taken as upper threshold requiring the demolition of the structures since repair is extremely difficult.

Table 3. Damage limit states for the bridge pier.

	Residual drift(%) limit state(j)				
Peak Drift(%) limit state (i)	**RD ≤ 0.25**	**0.25< RD ≤ 0.50**	**0.50< RD ≤ 0.75**	**0.75< RD ≤ 1.00**	**RD > 1.00**
MD ≤ 0.7	PL(1,1)	PL(1,2)	PL(1,3)	PL(1,4)	PL(1,5)
0.7 < MD ≤ 1.5	PL(2,1)	PL(2,2)	PL(2,3)	PL(2,4)	PL(2,5)
1.5 < MD ≤ 2.5	PL(3,1)	PL(3,2)	PL(3,3)	PL(3,4)	PL(3,5)
2.5 < MD ≤ 5	PL(4,1)	PL(4,2)	PL(4,3)	PL(4,4)	PL(4,5)
MD ≥ 5	PL(5,1)	PL(5,2)	PL(5,3)	PL(5,4)	PL(5,5)

6 **RESULTS AND DISCUSSION**

The probabilities of exceedance of various PLs with respect to the intensity measure (PGA) are computed. In this study, PGA is used as intensity measure because of its efficiency, sufficiency, practicality and computability in vulnerability assessment (Zhang and Huo 2009, Billah et al. 2013). The details of the PLs are given in Table 3. To elaborate, the probability of exceedance of PL(3,3) is the probability of MD>2.5 and RD>0.75. It is also to be noticed that PLs defined by a given maximum drift ratio limit with lower residuals might represent lesser damage state compared to the PLs with the same maximum drift limit combined with larger residual drift limits. Figure 3 shows the probability of exceedance corresponding to PL(3,2) and PL(4,2) for the SMA and steel RC bridge piers. It is interesting to note that while considering lower performance level, i.e. PL(3,2), the similar fragility can be observed in the both piers. However, differences between the two piers are distinctly visible at higher performance level PL(4,2). Figure 4 compares the fragility curves obtained for various PLs (PL(2,2), PL(3,2), PL(4,2), PL(5,2)) for SMA RC and steel RC bridge pier. Again it can be observed that the fragility of the SMA RC piers is relatively higher at lower PLs (PL(2,2)). However, as the higher PLs are considered performance of the SMA RC is improved. This result is because of the response of the Steel RC piers that is characterised by slightly lower MD and higher RD compared to the SMA RC piers. At lower PLs the pier response is within the elastic range or may incur small inelastic deformations with negligible residual deformations thus fragility curves of SMA RC are relatively higher than steel RC piers. As the residual displacement increases at higher PLs, due to the increase in inelastic deformations, the performance of the Steel RC piers gradually decreases in comparison to the SMA RC piers.

Table 3 presents the median value of the probability of exceedance at different PLs for two bridge piers. As shown at the lower PLs the median value for SMA RC is slightly lower compared to Steel RC suggesting better performance of Steel RC. At PL(3,3) the performance of both the piers in terms of the median value is nearly similar and at higher performance level the SMA RC outperforms the steel RC piers. It is interesting to note that median values for PL(5,1) for both piers are lower than that for PL(4,5). It should be noted that for a chosen system, at a given intensity level, fragility curve with the higher probability of exceedance indicates a lower damage state and vice versa. Therefore PL(5,1) defined by the higher MD with lower RD might represent a lesser damage state compared to PL(4,5) with slightly lower MD but significantly higher RD.

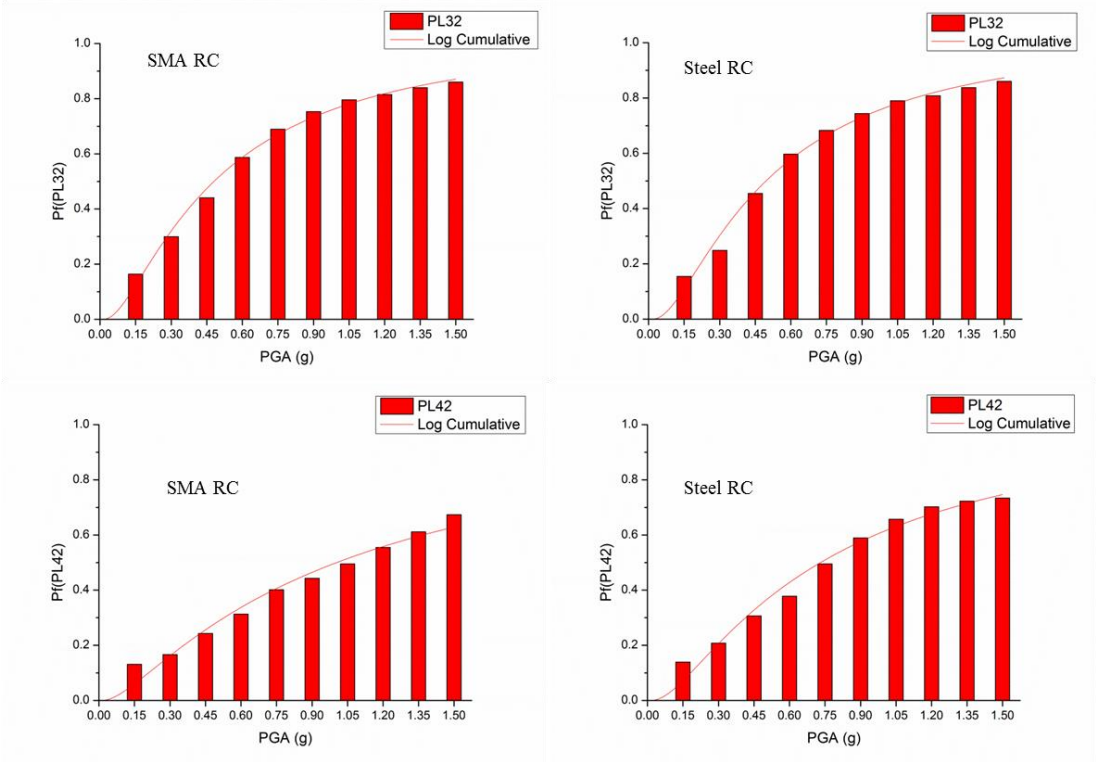

Figure 3. Probability of exceedance for PL (3,2) (top) and PL (4,2) (bottom) for the piers.

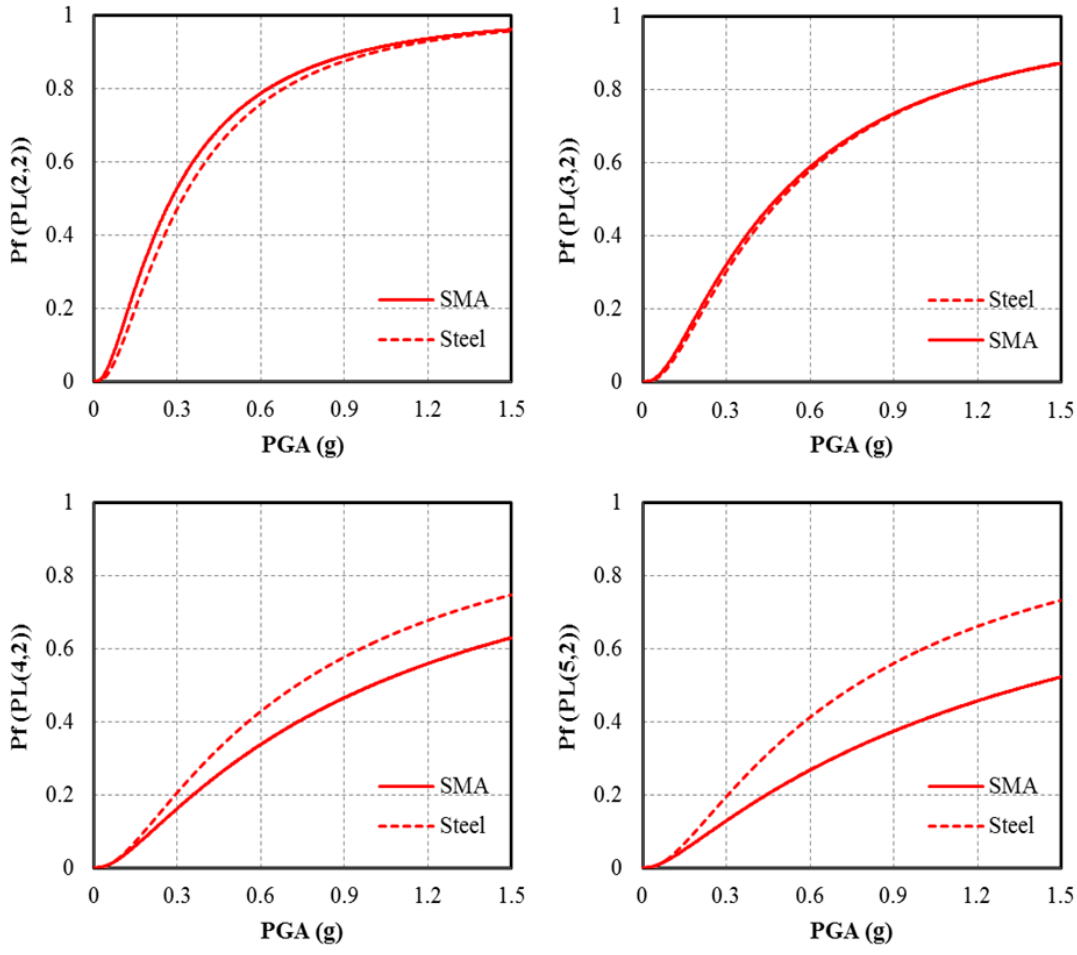

Figure 4. Fragility curves comparison at various PLs for the piers

Table 3. Comparison of median value of PGA for the bridge pier.

Piers	PL(1,1)	PL(2,2)	PL(3,2)	PL(3,3)	PL(4,2)	PL(4,5)	PL(5,1)
SMA RC	0.14	0.28	0.48	0.49	1.00	1.31	1.08
Steel RC	0.15	0.32	0.50	0.50	0.73	0.93	0.62

7 CONCLUSION

In this paper performance-based seismic assessment of SMA RC and steel RC bridge piers are made considering the combined maximum and residual deformations. Joint fragility curves, representing the probabilities of exceedance of PLs represented by a pair of MD and RD, are developed for the bridge piers. The results signify the need of considering the residual deformations in the performance of the structures. The results show that at lower PLs steel RC bridge piers with higher initial stiffness and energy dissipation capacity performs slightly better than the SMA RC bridge piers. However, the SMA RC bridge pier has the lower probability of exceeding higher damage level defined by combined maximum-residual deformations. The results advocate the benefits of using SMA reinforcement in the plastic hinge region of bridge piers constructed at moderate-high seismicity regions.

ACKNOWLEDGEMENT

The authors acknowledge the partial funding from Australian Research Council Linkage Project LP110200906 for carrying out this research.

REFERENCES:

Alam M.S., Youssef M.A., Nehdi M. 2010. Exploratory investigation on mechanical anchors for connecting SMA bars to steel or FRP bars. *Materials and Structures*. 43, 91-107.

Billah A.H.M.M., Alam M.S. 2014. Seismic Fragility Assessment of Concrete bridge piers reinforced with superelastic Shape memory Alloy. *Earthquake Spectra*. (Online version)

Billah A.H.M.M., Alam M.S., Rahman Bhuiyan M.A. 2013. Fragility Analysis of Retrofitted multicolumn bridge bent subjected to Near-fault and Far-field ground motion. *Journal of Bridge Engineering*. 18(10), 992-1004.

Billah A.H.M.M., Alam M.S. 2012. Seismic performance of concrete columns reinforced with hybrid shape memory alloy (SMA) and fibre reinforced polymer (FRP) bars. *Construction and Building Materials*. 28, 730-742.

Choi H., Saiidi M.S., Somerville P., El-Azazy S. 2010. An Experimental study of RC Bridge columns subjected to Near-fault ground motions. ACI *Structural Journal*. 107(1), 3-12.

Christopoulos C., Pampanin S., Priestley M.J.N. 2003. Performance-based seismic response of frame structures including residual deformations. Part I: Single-Degree-of-Freedom Systems. *Journal of Earthquake Engineering*. 7(1), 97-118.

Cruz Noguez C.A., Saiidi M. 2011. Shake table studies of a four-span bridge model with advanced materials. *Journal of Structural Engineering*. 138. 183-192.

Dutta A., Mander J.B. 1998. Seismic fragility analysis of highway bridges. Proceedings of the INCEDE-MCEER center-to-center workship on earthquake engineering fortiers in transportation systems. 311-325.

FEMA 273. 1997. NEHRP Guidelines for the Seismic Rehabilitation of Buildings. *Federal Emergency Management Agency*. Washington D.C., USA.

Japan Road Association. 2006. Specifications for Highway Bridges. JRA, Japan.

Kim S.H., Shinozuka M. 2007. Development of fragility curves of bridges retrofitted by column jacketing. *Probabilistic Engineering Mechanics*. 19, 105-112.

O'Brien M.,Saiidi M.S., Sadrossadat-Zadeh M. 2007. A Study of concrete bridge columns using innovative materials subjected to cyclic loading. *CCEER Report no. CCEER-07-01*. Dept. of Civil Engineering, University of Nevada, Reno, USA.

Pampanin S., Christopoulos C., Priestley M.J.N. 2002. Residual deformations in the performance based seismic assessment of frame structures. *Research Report ROSE-2002/02, European School of Advanced Studies in Reduction of Seismic Risk*. University of Pavia, Italy.

Pampanin S., Christopoulos C., Priestley M.J.N. 2002. Performance-based seismic response of frame structures including residual deformations. Part II: Multi-Degree-of-Freedom Systems. *Journal of Earthquake Engineering*. 7(1), 119-147.

Phan V., Saiidi M.S., Anderson J., Ghasemi H. 2007. Near Fault gournd motion effect on Reinforced concrete bridge columns. *Journal of Structural Engineering*. 133(7), 982-989.

Ramirez C.M., Miranda E. 2012. Significance of residual drifts in building earthquake loss estimation. *Earthquake Engineering and Structural Dynamics*. 41, 1477-1493.

Saiidi M.S., Ardakani S.M.S. 2012. An analystical study of residual displacement in RC bridge columns subjected to near-fault earthquake. *Bridge Structures*. 8. 35-45.

Saiidi M.S., Wang H. 2006. An Exploratory study of Seismic response of concrete columns with Shape memory alloy reinforcement. *ACI Structural Journal*. 103(3). 436-443.

Saiidi M.S., O'Brien M., Sadrossadat-Zadeh M. 2009. Cyclic response of concrete Bridge Column using Superelastic Nitinol and bendable concrete. *ACI Structural Journal*. 106(1). 69-77.

Seismosoft Inc. 2012. Seismo-struct- A computer program for static and dynamic nonlinear analysis of framed structures.

Shrestha B., Hao H. 2015. Parametric study of seismic performance of super-elastic shape memory alloy reinforced bridge piers. *Structures and Infrastructure Engineering*. (In press)

Shrestha K.C., Saiidi M.S., Cruz C.A. 2015. Advanced materials for control of post-earthquake damage in bridges. *Smart Materials and Structures*. 24(2), 025035.

Tazrav M., Saiidi M. 2013. Analytical studies of the seismic performance of a full-scale SMA reinforced bridge columns. *International Journal of Bridge Engineering*. 1. 37-50.

Tazrav M., Saiidi M. 2014. Reinforcing NiTi superelastic SMA for Concrete structures. *Journal of Structural Engineering*. 141(8). 04014197.

Uma S.R., Pampanin S., Christopoulos C. 2010. Development of Probabilistic Framework for Performance-Based Seismic Assesment of Structures considering Residual Deformations. *Journal of Earthquake Engineering*. 14(7), 1092-1111.

Vosooghi A., Saiidi M.S. 2010. Post-Earthquake evaluation and emergency repair of damaged RC bridge columns using CRRP materials. *CCEER Report no. CCEER-10-05*. Dept. of Civil Engineering, University of Nevada, Reno, USA.

Wehbe N., Saiidi M.S., Sander D. 1999. Seismic Performance of rectangular bridge column with moderate confinement. *ACI Structural Journal*. 96(2), 248-259.

Youssef M.A., Alam M.S., Nehdi M. 2008. Experimental Investigation on the seismic behaviour of beam-column joints reinforced with superelastic Shape Memory Alloy. *Journal of Earthquake Engineering*. 12(7). 1205-1222.

Zhang J., Huo Y. 2009. Evaluating effectiveness and optimum design of isolation devices for highway bridges using the fragility function method. *Engineering Structures*. 31(8), 1648-1660.